Theory and observation on non-linear effects limiting the coherence properties of high-Q hybrid Si/III-V lasers

Yaakov Vilenchik*[a], Christos T. Santis[b], Scott T. Steger[b], Naresh Satyan[c], Amnon Yariv[a,b]

[a]Applied Physics, California Institute of Technology, Pasadena, CA, USA
[b]Electrical Engineering, California Institute of Technology, Pasadena, CA, USA
[c]Telaris Inc., Santa Monica, CA, USA

ABSTRACT

Hybrid Si/III-V is a promising platform for semiconductor narrow-linewidth lasers, since light can be efficiently stored in low loss silicon and amplified in III-V materials. The introduction of a high-Q cavity in silicon as an integral part of the laser's resonator leads to major reduction of the laser linewidth. However, the large intra-cavity field intensity resulting from the high-Q operation gives rise to non-linear effects. We present a theoretical model based on non-linear rate equations to study the effect of two-photon absorption and induced free-carrier absorption in silicon on the laser's performance. The predictions from this model are compared to the experimental results obtained from narrow-linewidth lasers fabricated by us. It is shown to have an effect on the linearity of the L-I curve, and to reduce the achievable Schawlow-Townes linewidth.

Keywords: Two-photon absorption, TPA, Free-carrier absorption, FCA, Hybrid Si/III-V, Semiconductor lasers, Narrow linewidth lasers.

1. INTRODUCTION

The conventional semiconductor laser (SCL) design strategy that uses monolitically grown III-V materials for both electron and photon storage is fundamentally inconsistent with high coherence, i.e., narrow-linewidth, operation. Electrical current flows through the same volume which is occupied by the optical mode in order to inject carriers into the the quantum wells (QW). This imposes the use of optically-absorbing doped III-V layers which limit the achievable laser's quality factor (Q). Since the laser linewidth is proportional to Q^2, conventional SCLs are historically limited to sub-MHz linewidth.

Hybrid Si/III-V lasers have been demonstrated by several groups[1–4]. The main motivation for these devices is the generation of laser light on silicon platforms, close to high-speed silicon-based electronics or other silicon-photonics devices. In our case we use the silicon as part of the resonator and re-design the mode in such a way that the overwhelming majority (>97%) of the optical energy now resides in silicon. This results directly in orders of magnitude improvement in the resonator mode quality factor. It was recently demonstrated that this new design paradigm[4], shown in Fig. 1, is essential to minimizing spontaneous emission into the laser mode thus improving, by orders of magnitude, the coherence of the laser field. The losses in the Si rather than in the III-V now set the limit on coherence. The reduction in modal gain is precisely balanced by the reduction in modal loss, and laser conditions (gain = loss) are achieved without compromising threshold current.

Passive micro Si resonators with quality factors close to or bigger than a million were reported in the literature[4,5]. These integrated Si-based implementations yield small cavity sizes, compared to commercial low-linewidth lasers. The incorporation of such a high-Q Si resonator in the hybrid Si/III-V platform was demonstrated to yield lasers with linewidth as low as 18 KHz[4]. The high intra-cavity field intensities that are a consequence of the high-Q and the small cavity size enhance the probability of non-linear multi-photon processes. Two-photon absorption (TPA) and induced free-carrier absorption (FCA) were shown to alter the propagation of intense pulses[6], to suppress RIN[7] and to produce all-optical-modulation[8]. In this paper we investigate these non-linear processes in the context of high-Q semiconductor lasers.

*Send correspondence to: yasha@caltech.edu

Novel In-Plane Semiconductor Lasers XIV, edited by Alexey A. Belyanin, Peter M. Smowton, Proc. of SPIE
Vol. 9382, 93820N · © 2015 SPIE · CCC code: 0277-786X/15/$18 · doi: 10.1117/12.2078067

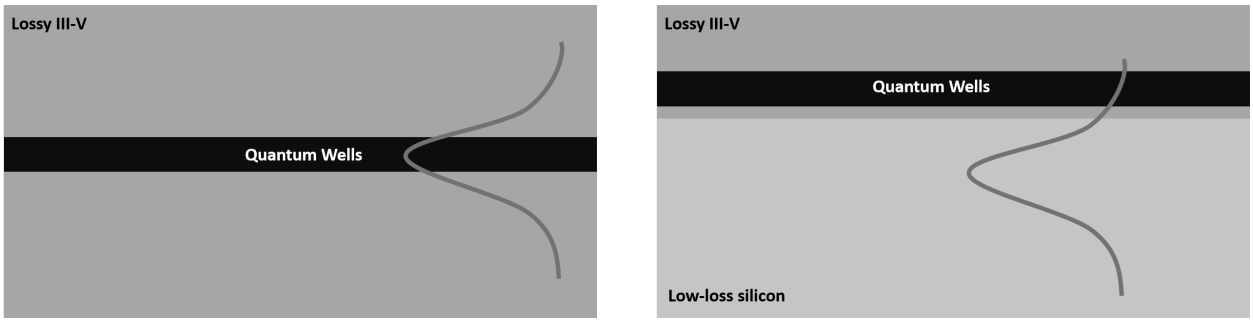

(a) (b)

Figure 1. (a) Conventional SCL design. (b) High Coherence Si/III-V design

2. THEORETICAL MODEL

Si has a large non-linear $\chi^{(3)}$ coefficient compared to commonly used low-loss materials such as SiO_2 or Si_3N_4. When the field intensity builds up in the presence of gain, non-linear processes, such as TPA and subsequent FCA, add extra loss[9], that would otherwise be negligible in the low-intensity passive version of the same resonator. In our laser design, in which the high optical energy is stored in a Si micro-resonator, the achievable cavity's quality factor may be limited due to non-linear loss.

We analyze the effect of these non-linear phenomena on the laser performance by including TPA and FCA in a modified version of the rate equations.

2.1 Flat mode approximation

In general, the optical mode and electron density profile vary along the resonator's volume. However, in order to numerically investigate non-linear laser-dynamics, it is advantageous to simplify the model. To that end, we neglect all spatial variations and approximate our mode as constant within a rectangular box. The size of the box will be equivalent to the FWHM volume of the mode, and the amplitude will be taken as the average amplitude within that rectangle.

The Electron density in the QWs will also be taken constant within a box. As shown in Fig. 2, two dimensions (x and z axes) of the electron-occupied volume will correspond to the optical cavity box, since we are only interested in the QW electrons that have significant contribution to the modal gain. The third dimension (y) will represent the thickness of the QW layer since the optical mode is approximately fixed over nm scale (compare to Fig. 1).

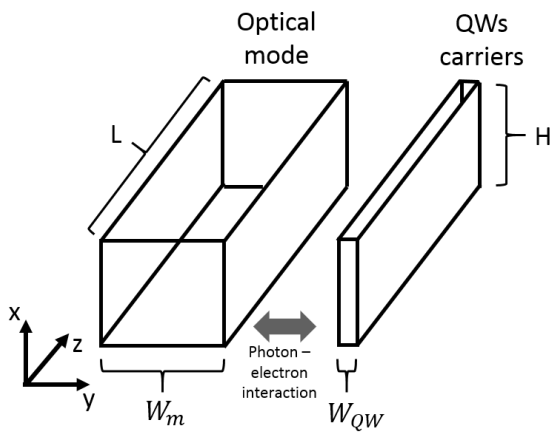

Figure 2. Flat mode approximation for the optical mode and the electron density

The interaction strength between photons and electrons will be calculated using the overlap integral for TE modes[10]:

$$\Gamma_i = \frac{\int_i n_i(\mathbf{r})|E(\mathbf{r})|^2 d^3\mathbf{r}}{n_{eff}\int_{all}|E(\mathbf{r})|^2 d^3\mathbf{r}} \tag{1}$$

Where n_{eff} is the mode's effective index, and the index i represents the desired region (QW in this case). The rate of generation (absorption) of the total number of photons N_p in the box will be calculated using the material gain (loss) G_m, which depends on the QW electron density n_e:

$$\frac{dN_p}{dt} = \Gamma_{QW} G_m(n_e) N_p \tag{2}$$

.

2.2 Two photon absorption

Optical Kerr effect in Silicon is responsible for intensity-dependant changes of the refractive index. TPA is manifested as the imaginary part of the index of refraction, and is non-zero whenever the photon's energy is larger than half the band-gap of silicon, as in the case of telecom wavelengths. TPA can be quantified using the coefficient β_T , which relates the change of the imaginary part of the refractive index Δn_i to the field's intensity I using:[11]

$$\Delta n_i = \frac{c}{2\omega}\beta_T I \tag{3}$$

Where c is the velocity of light, and ω is the angular optical frequency. The coefficient β_T is wavelength-dependent, and its value at $1.55\mu m$ has been measured by several authors[12–14] .

Optical loss induced by two-photon absorption can be described by a non-linear rate equation term for the average photon density n_p:

$$\frac{dn_p}{dt} = -\beta_T h\nu v_g^2 M_{TPA}\Gamma_{Si}^2 n_p^2 \tag{4}$$

Where $h\nu$ is the photon energy, v_g the group velocity and Γ_{Si} is the confinement factor in Si, defined as in eq. 1 with layer i being the Si layer. The factor M_{TPA} captures the difficulty of describing non-linearities using a flat average-intensity model: Since TPA is proportional to the local density *squared*, it is much stronger at the mode's local peak than at its average over the modes volume V_p. M_{TPA} is defined to ascertain the flat-mode-approximation of section 2.1 will not yield gross under-estimation of TPA processes:

$$M_{TPA} = V_p \frac{\int_{Si}|E(\mathbf{r})|^4 d^3\mathbf{r}}{\left(\int_{Si}|E(\mathbf{r})|^2 d^3\mathbf{r}\right)^2} \tag{5}$$

2.3 Free carrier absorption

For each TPA absorption event in Si, an electron-hole pair is generated. Long carrier recombination life time of conduction-band electrons in intrinsic silicon allows these carriers to accumulate and interact with the electromagnetic field. This interaction induces both extra loss through plasma effect FCA and refractive index changes. The strength of these effects can be well modeled using the Drude model[15] where the loss coefficient per unit distance α_{FCA} and refractive index change n_{FCA} can be directly related to the electron and hole concentrations n_{Si} and p_{Si} respectively. For intrinsic silicon we can use the parameter[11] σ_a to relate loss rate to electron concentration:

$$\alpha_{FCA} = \sigma_a n_{Si} \tag{6}$$

The changes in refractive index due to free carriers in Si, at $\lambda = 1550$nm, can be described using[11]:

$$n_{FCA} = -8.8\cdot 10^{-22} n_{Si} - 8.5\cdot 10^{-18} p_{Si}^{0.8} \tag{7}$$

To estimate the number of free electrons in the steady state operation of the laser we need to solve the diffusion-recombination-generation equation for our specific waveguide geometry. As the bulk recombination time of Si is

in the order of a few μsec , the lifetime will be dominated by surface and interface recombination. For a typical laser bar of length and width of a few millimeters, we can neglect surface recombination from distant facets and edges of the bar. The dominant source of electron annihilation would be surface recombination along the interface of the Si slab, which is of sub-micrometers thickness. Therefore we can approximate the 3-dimensional structure using a two dimensional equation[16] :

$$\frac{dn_{Si}}{dt} = \frac{\beta_T h\nu v_g^2}{2} n_p^2 - \frac{n_{Si}}{\tau_b} + D_a \frac{d^2 n_{Si}}{dx^2} - 2\frac{S}{H} n_{Si} \tag{8}$$

Where τ_b is the bulk recombination lifetime in Si, D_a is the ambipolar diffusion coefficient, S is the surface recombination velocity and H is the Si slab thickness. Once we have numerically solved this equation for given photon density profile we can define an effective lifetime for carriers in Si for the given optical mode:

$$\tau_{eff} = \frac{2}{\beta_T h\nu v_g^2 n_p^2} \frac{\int n_{Si}(x) n_p(x) dx}{\int n_p(x) dx} \tag{9}$$

The parameter τ_{eff} describes the average time in which generated electrons interact with the optical mode before they recombine at the surface, the bulk or diffuse away from the mode's area. For micro scale structures the exact value of this parameter is usually dominated by the quality and size of surfaces and interfaces in Si. Typical values in the literature are around $\tau_{eff} = 1$ns.[16] However, since high-Q resonators require high quality interfaces and etched surfaces we expect the effective lifetime to be higher than the normally encountered values.

2.4 Modified rate equations

The SCL rate equation can now be modified to take into account TPA and FCA. Since TPA is a non-linear process that scales with the intensity of the light in the cavity, rather then the total photon energy, it is natural to express the rate equations in terms of the electron and photon densities. In the total numbers description the stimulated emission process conserves electrons/photons, i.e., radiative recombination of one QW electron generates exactly one photon, and vice versa. Referring to Fig. 2, the rate of the total electron and photon number can be converted to densities by dividing by the volume of the QW and optical cavity respectively. It is useful to define a geometrical confinement factor:

$$\Gamma_{geom} = \frac{W_{QW}}{Wm} \tag{10}$$

The low losses due to the high-Q resonator enables the laser to operate close to transparency. This allows us to write the material gain using the approximate linear expression:

$$G_m = 2v_g G_m^{'}(n_e - n_{tr}) \tag{11}$$

without losing much accuracy. $G_m^{'}$ is the material differential gain and n_{tr} is the transparency carrier density. The optical energy loss rate α in the cavity is expressed using the loaded quality factor Q:

$$\alpha = \frac{2\pi\nu}{Q} \tag{12}$$

The reduced QW confinement factor Γ_{QW} , which is a characteristic of our high-Q platform, minimizes spontaneous emission rate into the mode. The rate can be expressed as:

$$R_{sp} = \frac{\Gamma_{QW} G_m(n_e) n_{sp}}{V_p} \tag{13}$$

Where V_p is the effective mode volume and n_{sp} is the population inversion factor. Eq. 13 is a consequence of a fundamental relationship between stimulated and spontaneous emission[17] .

We can now express the systems of rate equations as:

$$\frac{dn_e}{dt} = -\frac{n_e}{\tau_r} - \frac{\Gamma_{QW}}{\Gamma_{Geom}} G_m(n_e) n_p + \frac{\eta I}{qV_{QW}} \tag{14}$$

$$\frac{dn_p}{dt} = \left(\Gamma_{QW} G_m(n_e) - \alpha\right) n_p - \beta_T h\nu v_g^2 M_{TPA} \Gamma_{Si}^2 n_p^2 - v_g \sigma_a n_{Si} \Gamma_{Si} n_p + R_{sp} \tag{15}$$

$$\frac{dn_{Si}}{dt} = \frac{1}{2}\beta_T h\nu v_g^2 M_{TPA} \Gamma_{Si} n_p^2 - \frac{n_{Si}}{\tau_{eff}} \tag{16}$$

The parameters used for the rate equations analysis are summarized in table 1.

Parameter	Description	Value	Units
τ_r	Recombination life time (including non-radiative recombination)	$50 \cdot 10^{-9}$	sec
G_m	Material gain	eq. 11	sec^{-1}
$G_m^{'}$	Differential material gain	$1 \cdot 10^{-19}$	m^2
n_{tr}	QWs transparency density	$2 \cdot 10^{24}$	m^{-3}
η	Quantum efficiency (including current leakage)	0.3	-
I	Pump current	(sweep)	Amper
q	Electron charge	$1.6 \cdot 10^{-19}$	Coulombs
V_{QW}	Quantum well effective volume	$4.2 \cdot 10^{-17}$	m^3
V_p	Effective mode volume	$6 \cdot 10^{-16}$	m^3
α	Linear loss rate in the cavity	eq. 12	sec^{-1}
Γ_{QW}	QW confinenmt factor	eq. 1	-
Γ_{geom}	Geometrical confinement factor	0.07	-
v_g	Mode's group velocity	$c/3.53$	$\frac{\text{m}}{\text{s}}$
β_T	TPA coefficient	$5 \cdot 10^{-1212-14}$	$\frac{\text{m}}{\text{W}}$
M_{TPA}	TPA magnification factor	eq. 5	-
σ_a	FCA cross section	$1.45 \cdot 10^{-2111}$	m^2
Γ_{Si}	Si confinement factor	eq. 1	-
R_{sp}	Spontaneous emission rate into mode	eq. 13	sec^{-1}
τ_{eff}	Si carriers effective lifetime	$30ns^*$	sec

Table 1. Parameters used for rate equations

3. STEADY STATE SOLUTION

The non-linear rate equations 14, 15 and 16 can be solved in the steady state by setting all $\frac{d}{dt} = 0$. The numerical solution of the system of equations can provide insights on the effect of TPA and FCA on laser performance.

3.1 LI curve

Output coupling of lasers with different resonators' quality-factors can in general vary. Even in lasers with the same intrinsic Q, the mirror grating can be adjusted to change the total Q, and the output coupling. In order to compare different laser designs, we will assume that each laser has a known intrinsic quality-factor, and that the mirror grating is designed for critical output coupling (intrinsic Q = external Q). As the intra-cavity intensity builds up, TPA and FCA processes become more and more dominant, and introduce excess loss. The rate of this non-linear loss would increase with increasing pump current and would yield a non-linear L-I curve, as can be seen in Fig. 3.

*Measured experimentally. Measurement technique is beyond the scope of this paper.

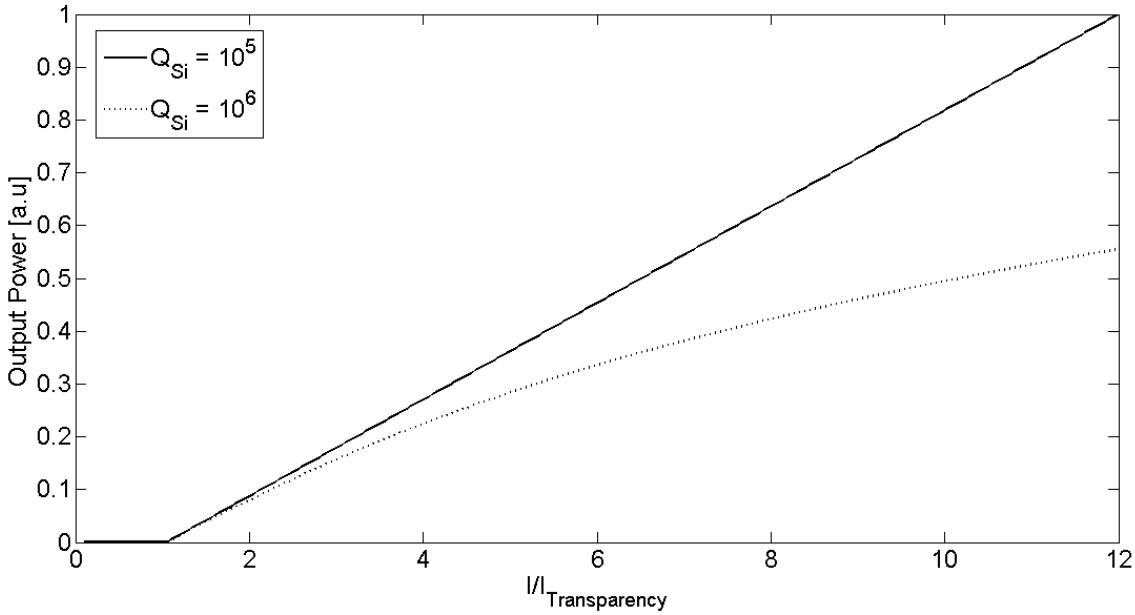

Figure 3. Theoretical L-I curves for different resonator quality factors

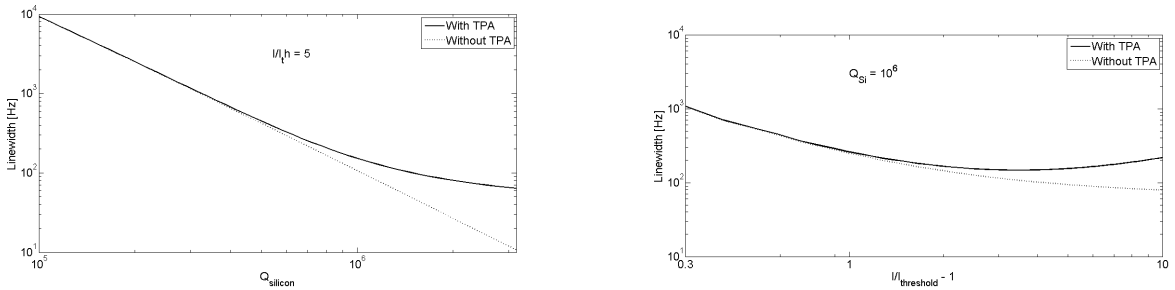

(a) (b)

Figure 4. Effect of TPA on linewidth. (a) ST linewidth vs. Q with and without TPA at 5 times threshold. (b) ST linewidth vs. injection current with and without TPA at Q=10^6

3.2 Linewidth

The Schawlow–Townes (ST) Linewidth[18] is well understood, and known to be inversely proportional to Q^2 and to the output power. For laser resonator with nominally high quality factor the non-linear loss effectively limits the Q by introducing excess intensity-dependant loss, thus preventing the intra-cavity intensity from rising. As demonstrated in Fig. 4(a), this effect broadens the linewidth compared to the ST linewidth.

The saturation of stored energy due to TPA and FCA also occurs when the pump current increases, as can be seen in Fig. 3. As a consequence, the linewidth would decrease at a smaller rate than the expected I^{-1}. This can be seen in Fig. 4(b). At high currents TPA causes re-broadening of the linewidth with increased pump current. This is due to the increased total loss by TPA and FCA - the gain has to compensate for the excess non-linear loss by increasing the QW carrier density. This, in turn, increases the spontaneous emission rate into the mode. This effect is accompanied by the saturation of the stored energy in the cavity to broaden the linewidth at higher currents.

4. EXPERIMENTAL RESULTS

We have fabricated ultra narrow-linewidth lasers on the hybrid Si/III-V platform. The high-Q Si resonator was implemented using a 1-D modulated photonic grating. A distributed defect was used to support a high-Q mode

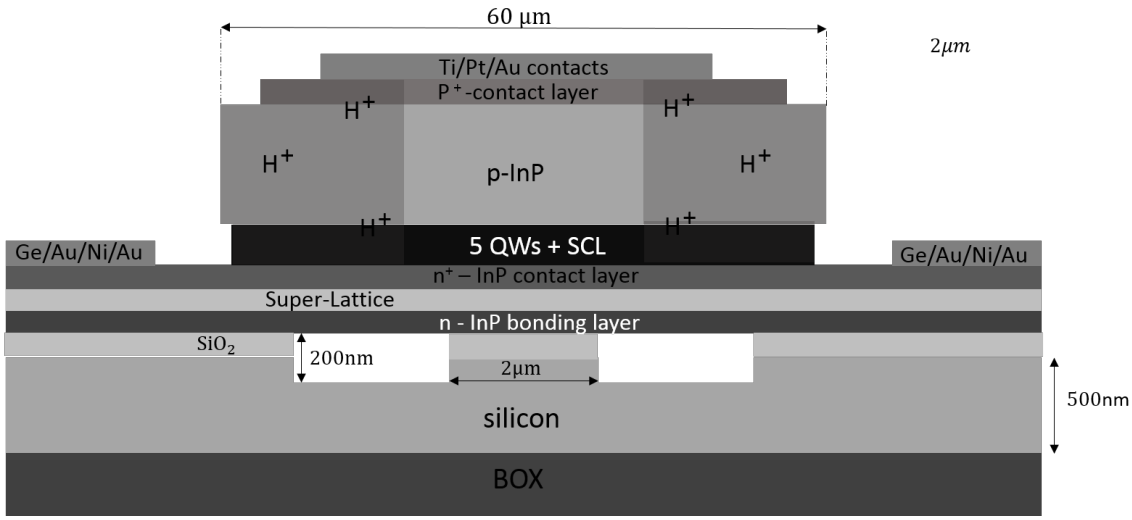

Figure 5. Schematics of the fabricated lasers (not to scale)

with low radiation losses. This design and fabrication process has yielded [4] resonators of Q as high as 10^6.

Unpatterend III-V epi-structure (InP substrate, InGaAsP QWs) was bonded to the high-Q Si resonator using direct bonding at 285 °C under pressure of 205 PSI. An 8μm current channel was defined using photolithography followed by proton implantation. P-contact metal pads were deposited using lift-off lithography and Ti/Pt/Au e-beam evaporation. Wet chemical Mesa etch followed by n-metal Ge/Au/Ni/Au e-beam evaporation was performed to define the n-contact metal pads. The total Q-factor of the hybrid Si/III-V structure was controlled by modal engineering: Due to the high-Q Si resonator, the degree of overlap of the mode with the higher loss III-V was used to control the total Q. A schematic of the device is shown in Fig. 5, however, the exact design and fabrication details are beyond the scope of this paper.

Lasers of two different quality factors were fabricated and measured. The devices were pumped and output light was collected using an integrating sphere. Fig. 6 compares between LI curves of lasers of an estimated Q of 10^5 and $3 \cdot 10^5$. The lower-Q device was measured using a CW current source, while the other device was measured using a pulsed current source. The pulsed current source was used to avoid misinterpretation of thermal roll-off as TPA, since thermal effects might cause the same non-linearity. The short pulse width of $1\mu s$ and duty cycle of 1% ensures that thermal effects are minimal. The L-I curve for the pulsed current source (Fig. 6, solid line) was normalized using the duty cycle, for comparison with the CW measurement (dashed line). The higher-Q device clearly shows a non-linear LI curve, a signature of TPA and subsequent and FCA.

The power spectral density of the frequency noise was measured using an unbalanced Mach-Zehnder interferometer with FSR of 1.56 GHz, and a balanced PD. A feedback loop was used to lock the piezo-driven MZI such that it is in quadrature during the measurement. The Schawlow–Townes linewidth of lasers with the high quality factor was lower than our spectral measurement setup noise floor, and could not be measured. Due to the high-Q operation, the ST white noise floor was masked by $1/f^{\alpha}$ technical noise. Therefore, an experimental equivalent of Fig. 4 could not be produced. However, the high $1/f^{\alpha}$ spectral shape that masked the ST white noise floor can be explained by refractive index fluctuations induced by free-carriers in Si, that are a consequence of TPA. The mathematical justification of this statement is beyond the scope of this paper.

5. SUMMARY

We have studied the effect of two-photon absorption and subsequent free-carrier absorption on the performance of ultra-narrow linewidth hybrid Si/III-V lasers. It was found that these non-linear effects induce a power-dependent reduction of the total cavity quality factor, thus yielding non-linear L-I curves, and reducing the achievable linewidth. The predictions from a non-linear rate equation model were verified experimentally using hybrid Si/III-V lasers of expected quality factor of $3 \cdot 10^5$.

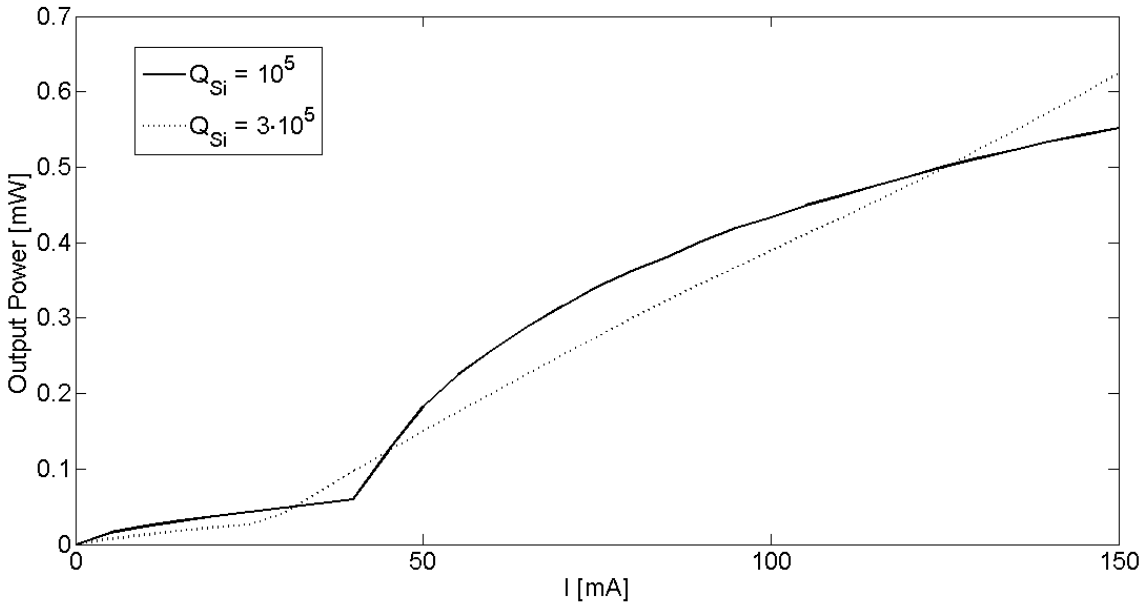

Figure 6. Experimental L-I curve for lasers of different quality factors

ACKNOWLEDGMENTS

This work was supported in part by the Defense Advanced Research Projects Agency and the Army Research Office. The authors would like to thank the Kavli Nanoscience Institute at the California Institute of Technology for providing technical and fabrication infrastructure.

REFERENCES

1. H. Park, A. Fang, S. Kodama, and J. Bowers, "Hybrid silicon evanescent laser fabricated with a silicon waveguide and III-V offset quantum wells," *Opt. Express* **13**, pp. 9460–9464, Nov 2005.
2. S. Stankovic, R. Jones, M. Sysak, J. Heck, G. Roelkens, and D. Van Thourhout, "Hybrid III-V/Si distributed-feedback laser based on adhesive bonding," *Photonics Technology Letters, IEEE* **24**, pp. 2155–2158, Dec 2012.
3. K. Tanabe, K. Watanabe, and Y. Arakawa, "III-V/Si hybrid photonic devices by direct fusion bonding," *Sci. Rep.* **2**, pp. –, Apr. 2012.
4. C. T. Santis, S. T. Steger, Y. Vilenchik, A. Vasilyev, and A. Yariv, "High-coherence semiconductor lasers based on integral high-Q resonators in hybrid Si/III-V platforms," *Proceedings of the National Academy of Sciences* **111**(8), pp. 2879–2884, 2014.
5. A. Griffith, J. Cardenas, C. B. Poitras, and M. Lipson, "High quality factor and high confinement silicon resonators using etchless process," *Opt. Express* **20**, pp. 21341–21345, Sep 2012.
6. E.-K. Tien, N. S. Yuksek, F. Qian, and O. Boyraz, "Pulse compression and modelocking by using tpa in silicon waveguides," *Opt. Express* **15**, pp. 6500–6506, May 2007.
7. A. E. Amili, G. Kervella, and M. Alouini, "Experimental evidence and theoretical modeling of two-photon absorption dynamics in the reduction of intensity noise of solid-state Er:Yb lasers," *Opt. Express* **21**, pp. 8773–8780, Apr 2013.
8. D. Moss, L. Fu, I. Littler, and B. Eggleton, "Ultrafast all-optical modulation via two-photon absorption in silicon-on-insulator waveguides," *Electronics Letters* **41**, pp. 320–321, March 2005.
9. P. Barclay, K. Srinivasan, and O. Painter, "Nonlinear response of silicon photonic crystal microresonators excited via an integrated waveguide and fiber taper," *Opt. Express* **13**, pp. 801–820, Feb 2005.

10. T. Visser, H. Blok, B. Demeulenaere, and D. Lenstra, "Confinement factors and gain in optical amplifiers," *Quantum Electronics, IEEE Journal of* **33**, pp. 1763–1766, Oct 1997.
11. Q. Lin, O. J. Painter, and G. P. Agrawal, "Nonlinear optical phenomena in silicon waveguides: modeling and applications," *Opt. Express* **15**, pp. 16604–16644, Dec 2007.
12. M. Dinu, F. Quochi, and H. Garcia, "Third-order nonlinearities in silicon at telecom wavelengths," *Applied Physics Letters* **82**(18), pp. 2954–2956, 2003.
13. H. K. Tsang, C. S. Wong, T. K. Liang, I. E. Day, S. W. Roberts, A. Harpin, J. Drake, and M. Asghari, "Optical dispersion, two-photon absorption and self-phase modulation in silicon waveguides at 1.5um wavelength," *Applied Physics Letters* **80**(3), pp. 416–418, 2002.
14. J. Zhang, Q. Lin, G. Piredda, R. W. Boyd, G. P. Agrawal, and P. M. Fauchet, "Anisotropic nonlinear response of silicon in the near-infrared region," *Applied Physics Letters* **91**(7), pp. –, 2007.
15. R. A. Soref and Bria, "Electrooptical effects in silicon," *IEEE Journal of Quantum Electronics* **QE-23**, pp. 123–129, January 1987.
16. D. Dimitropoulos, R. Jhaveri, R. Claps, J. C. S. Woo, and B. Jalali, "Lifetime of photogenerated carriers in silicon-on-insulator rib waveguides," *Applied Physics Letters* **86**(7), pp. –, 2005.
17. A. Yariv, *Quantum electronics*, Wiley, 3rd ed., 1989.
18. A. L. Schawlow and C. H. Townes, "Infrared and optical masers," *Phys. Rev.* **112**, pp. 1940–1949, Dec 1958.